Republic of Algeria Democratic and People's
Ministry of Higher Education and Scientific

Kasdi Merbah Ouargla University
Faculty of Applied Sciences
Department of Mechanical Engineering

Dissertation
Presented to obtain a diploma of

MASTER

Branch: Mechanical Engineering
Specialty: Energetic
Presented by:
Naam Hibet Errahmane

Theme

Improving the Efficiency of the VASIMR Engine for Space Vehicles

Publicly supported on: 12/06/2024

In front of the jury:

Recioui Bakhta	MCA	President	UKM OUARGLA
Baatouche Mouna	MAA	Examiner	UKM OUARGLA
Naam Amel	Prof	Supervisor	UKM OUARGLA

Academic year:2023/2024

Dedication

I dedicate this thesis to my beloved mother for her unwavering love, support, and guidance throughout my academic journey; my late father, whose memory continues to inspire me to strive for excellence; my brothers, for always believing in me and cheering me on; and all those who have supported me along the way. Your encouragement has meant the world to me.

THANKS AND APPRECIATION

Thank God, we've been blessed with success and repayment.

Dear esteemed Professors , As I stand here on the brink of a new chapter, I am filled with gratitude towards each and every one of you for your unwavering support, guidance, and dedication throughout my academic journey. Today, as I reflect on the monumental achievement of graduating, I cannot help but acknowledge the pivotal role that all of you have played in my success.

Supervising Naam Amel Your mentorship has been nothing short of inspiring. Your wisdom, patience, and expertise have shaped not only my academic pursuits but also my personal growth. You have challenged me to push beyond my limits, to think critically, and to strive for excellence. Your belief in me has been a source of strength, and for that, I am eternally grateful.

We also thank the board of examiners: President Recioui Bakhta, and Examiner Baatouche Mouna for their acceptance to judge our work.

Contents

General introduction: 7

1 Vasimr engine **9**

1.1 Introduction: 9

1.2 Discovering life on Mars: 9

1.3 Proposed work on VASIMR and current research on its engine: 10

1.4 Anatomy of the VASIMR engine: 12

1.4.1 Injection Stage (Helicon Discharge): 13

1.4.2 The Heating Stage (ICRH-Ion Cyclotron Resonance Heating): 16

1.4.3 Magnetic Nozzle: 21

1.5 Performance of VASIMR: 21

1.6 Conclusion: 22

2 Generality on plasmas **24**

2.1 Introduction: 24

2.2 Degree of ionization: 24

2.3 Plasma Parameters: 25

2.3.1 Plasma Frequency: 25

2.3.2 Debye Length: 25

2.3.3 Landau length: (Critical length of binary interaction): 26

2.3.4 Ratius of the ionic sphere: 26

2.3.5 Electronic sphere radius: 26

2.3.6 De Broglie Thermal Wave Length: 27

2.4 Plasma in a constant uniform magnetic field: 27
2.5 Conclusion: 30

3 Results and discussions **31**
3.1 Introduction: 31
3.2 The VASIMR thruster (VF-24): 31
3.2.1 The influence of the volume dimensions: 32
3.2.2 The influence of both density and temperature: 33
3.2.3 The influence of the atomic number: 34
3.3 Power in work of A.V. Ilin and al: 34
3.4 Conclusion: 35
General conclusion: 36

List of Tables

1.1 Some properties and parameters of the four propellants used in plasma VASIMR engine. 15

1.2 Comparisons between some experimental results of antenna geometry. 19

3.1 Interesting typical values of operating parameters for 24 kW VASIMR thruster. . 32

3.2 Interesting typical values of operating parameters for 24 kW VASIMR thruster. . 34

List of Figures

1-1 The suggested rocket architecture with descending vehicle. 11

1-2 Anatomical schematic of magnetoplasma rocket (VASIMR) engine. 12

1-3 Different parts of VASIMR engine. 13

1-4 Schematic showing the position of the two RF generators in the VASIMR® VX-200. 14

1-5 Moog type flow controller. 16

1-6 Steady-state of the actual discharge source of the helicon. 17

1-7 Actual source of Helicon antenna. 17

1-8 Actual image of the ICRH antenna in VASIMR. 18

1-9 Some previous improvement for ICRH antenna. 19

2-1 Helicoidal trajectory for ρ Larrnor radius, and θ angle of inclination. 29

3-1 Evolution of percentage $L_e(\%)$ as a function of volume parameters $r_{\min}$ and x in the case where $n_a = 2.10^{18}\,\mathrm{m}^{-3}$, $T_e = 1.16 \times 10^5$ K, and $z = 7$. 37

3-2 Evolution of percentage $L_i(\%)$ as a function of volume parameters $r_{\min}$ and x in the case where $n_a = 2.10^{18}\,\mathrm{m}^{-3}$, $T_i = 1.16 \times 10^6\,\mathrm{K}$, and $z = 7$. 38

3-3 Variation of percentage $L_e(\%)$ as a function of electronic temperature T_e and density n_a in the case where $r_{\min} = 0.6\,\mathrm{m}$, $x = 0.02$ m, and $z = 7$. 39

3-4 Variation of percentage $L_i(\%)$ as a function of ionic temperature T_i and density n_a in the case where $r_{\min} = 0.6\,\mathrm{m}$, $x = 0.02$ m, and $z = 7$. 40

3-5 Evolution of percentage $L_e(\%)$ as a function of atomic number Z in the case where $n_a = 2.10^{18}\,\mathrm{m}^{-3}$, $T_e = 1.16 \times 10^5$ K, $r_{\min} = 0.6\,\mathrm{m}$, $x = 0.02$ m. 41

3-6 Evolution of percentage $L_i(\%)$ as a function of atomic number Z in the case where $n_a = 2.10^{18}\,\mathrm{m}^{-3}$, $T_i = 1.16 \times 10^5$ K, $r_{\min} = 0.6\,\mathrm{m}$, and $x = 0.02$ m. 42

List of Abbreviations

VASIMR	.....	Variable Specific Impulse Magneto plasma Rocket.
MIT	.....	Plasma Fusion Center.
NASA	.....	National Aeronautics and Space Administration.
ICRH	.....	Ion Cyclotron Resonance Heating.
MOC	.....	Mars Orbiter Camera.
RF	.....	Radio Frequency.
DC	.....	Direct Current.
EP	.....	Electric Propulsion.
BSCCO	.....	Bismuth StrontiumCalcium Copper Oxide.

0.1 General introduction:

Modern man has always dreamed of finding another planet with life. The discovery of Mars atmospheric conditions in 2001 opened the scope for discovering life on Mars. To carry out space missions and perform distant journeys in our deep space in a short time, we need a fast vehicle. Thus, an electromagnetic propulsion rocket has been designed called VASIMR. Scientists led by astronaut Franklin Chang Díaz have been working on creating a quicker propulsion system for space flight since the 1970s, first at MIT and then at NASA [1, 2]. The NASA Johnson Space Center's Advanced Space Propulsion Lab has been developing the Variable Specific Impulse Magnetoplasma Rocket (VASIMR) for a number of years.

The specific impulse and a gas's exit velocity are intimately correlated. The energy of the chemical bonds in the propellant is taken from the exhaust, placing an upper limit on the exhaust velocity—this is a fundamental constraint of chemical rockets. Therefore, accelerating the propellant using a different technique is required to produce a rocket with a high specific impulse [3].

The idea behind electric propulsion (EP) is to accelerate the propellant with electrical energy instead of chemical energy. Based on the propellant acceleration mechanism, EP devices fall into three categories: electromagnetic, electrostatic, and electrothermal. Ohmic heating via a resistor or an electrical arc increases the propellant's enthalpy, which expands the gas through a nozzle to produce thrust in electrothermal rockets. Ionizing the propellant, electrostatic and electromagnet thrusters use electric fields or the Lorentz force, respectively, to accelerate the ions and produce thrust [4]. The underlying idea of all EP devices is that propellant exhaust energy is deposited from an external power source rather than being taken from internal energy. This suggests that the specific impulse is limitless, even though spacecraft design really places restrictions on it.

To control the efficiency in the VASIMR, we should estimate the power ratio, which is the output power (the magnetic nozzle power) divided by the input power (the RF power of the helicon and ICRH systems) [5, 6]. The power loss is taken into consideration in determining the total input power.

What matters to us in developing the VASIMR is to increase its speed and thus control its efficiency. In our present work, we try to find a new improvement in efficiency for the VASIMR engine.

In the first chapter, we will present general information about VASIMR, historical development, proposed work, and current research. We will give some details of engine and its anatomy, as well as its components and stages.

In the second chapter, we will describe the plasma medium and define its parameters. We will also present the plasma behavior in a constant, uniform magnetic field.

To present our improvement on the VASIMR efficiency in the third chapter, we will apply our result on the 24 kw VASIMR. We will treat some ranges of parameters and extract good conditions that make the efficiency as strong as possible.

Chapter 1

Vasimr engine

1.1 Introduction:

In order to maintain the satellites and perform distant journeys in our deep space in a fast way, an electromagnetic propulsion rocket has been designed called VASIMR. Scientists led by astronaut Franklin Chang Díaz have been working on creating a quicker propulsion system for space flight since the 1970s, first at MIT and then at NASA. In this chapter, we have focused on the main components of the VASIMR engine: the helicon plasma source, the magnetic nozzle, and the ICRH. In the helicon stage, the plasma is created by a radio frequency wave, while in the ICRH stage, the plasma is heated in order to expand and perform a thrust at the magnetic nozzle. In addition, we have described the main previous missions to Mars and discussed the condition and possibility of life on it. We have presented, on the other hand, the proposed work on VASIMR and current research on the VASIMR engine to discover in general the space, in particular, life on Mars.

1.2 Discovering life on Mars:

Modern man has always dreamed of finding another planet with life. The discovery of Mars atmospheric conditions in 2001 opened the scope for discovering life on Mars, with the NASA Mars Odyssey program contributing to numerous science results. The program mapped chemical elements, minerals, hydrogen distribution, and water ice in the Polar Regions, and recorded

radiation environments in low Mars orbit. The 2001 Mars Odyssey has produced a wealth of scientific findings. The quantity and distribution of the minerals and chemical components that make up the surface of Mars have been mapped. Scientists have found massive amounts of water ice buried just below the surface in the Polar Regions thanks to maps showing the distribution of hydrogen. In order to assess the radiation risk to potential future human explorers who may visit Mars, Odyssey has also documented the radiation environment in low Mars orbit [1]. But, When a robotic lander touched down on Mars, it was unable to find any signs of life. Projects to find life on Mars are still being worked on. Among the more than 40 missions that were sent to Mars, only a few were successful in achieving their purposes. Mariner 4 was the first mission to be successful in 1964 to capture 21 images, while Phoenix took 25 gigabits of photos in 2007. The majority of our knowledge about Earth's history comes from the study of layered rocks and the components, structures, and fossils that can be discovered there. Throughout craters and chasms on the red planet, outcrops of stratified rock exposed by faulting and erosion have been seen in hundreds of mars orbiter camera (MOC) photos.

1.3 Proposed work on VASIMR and current research on its engine:

Both liquid and solid rockets are frequently utilized for space missions. Although these two varieties are less expensive than others, they are not suitable for missions requiring the long-distance transportation of large structures and heavy loads. Furthermore, they lack the efficiency of nuclear thermal rockets and variable specific impulse magnetoplasma rockets (VASIMR).

A VASIMR is recommended for a Mars expedition due to its very efficient feature. The suggested rocket architecture with descending vehicle is seen in figure (1-1). In addition, the rocket has an orbiter on board to send the data back to Earth.

The VASIMR concept was developed by scientist and former astronaut Franklin Chang-Diaz, who has been working on its development since 1977. When he was researching magnetic ducts and their potential for controlled nuclear fusion, the concept occurred to him. Since then, research and development have been done on the VASIMR rocket. Franklin Chang-Diaz founded the Ad Astra Rocket Company in January 2005 to start developing the VASIMR engine

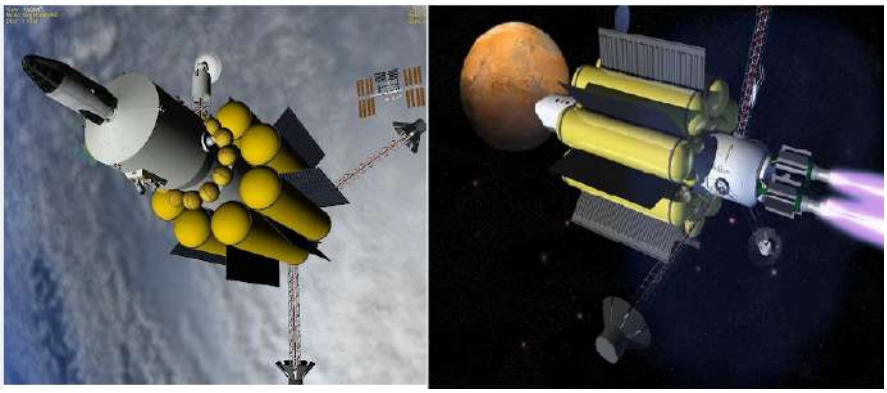

Figure 1-1: The suggested rocket architecture with descending vehicle.

following years of study at NASA. Control over the Advanced Space Propulsion Laboratory was given to the Company. They built a 100 kW version after the initial 50 kW prototype. The most recent test run for a 200 kW engine was completed satisfactorily [3].

The initial VASIMR engine, type VX-50, demonstrated a thrust capacity of 0.5 newtons. Data from the corporation indicated that the VASIMR efficiency at that time was 67%. The efficiency of the VX-50 engine, which can process 50 kW of total radio frequency power, was reported to be 59% in published statistics. It was thought that increasing power levels would boost the engine's overall efficiency.

The most recent details regarding the development of VX-200 were made public in a news release on November 23, 2010. It has effectively reached an exhaust speed of 50 km/ s, a thrust force of 5.7 N, and a VASIMR efficiency of 72%. This article describes the current 200 kW engine findings that led to the 2013 International Space Station mission [4].

At a fraction of the cost of chemical technologies, the engine is anticipated to carry out the following tasks:

- Space station drag compensation.
- Delivery of cargo to the moon.
- Repositioning satellites - Refueling, maintaining, and repairing satellites.
- In the retrieval of space resources.
- Extremely quick robotic expeditions in distant space.

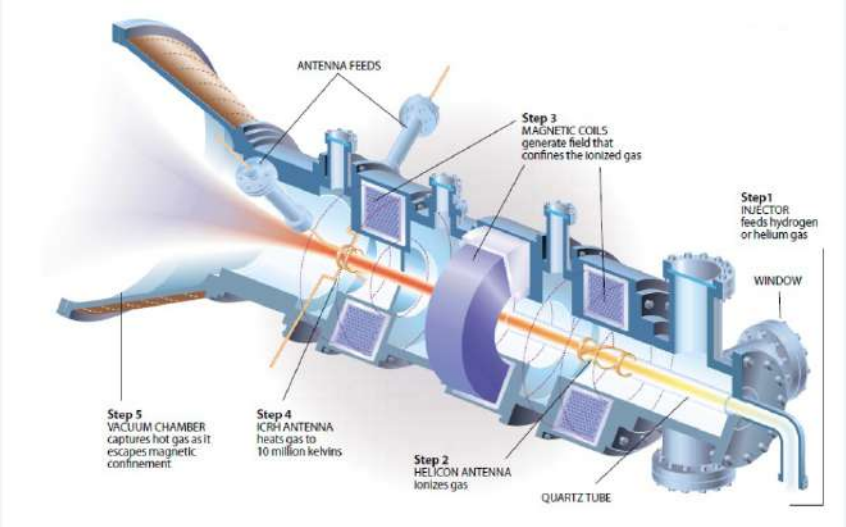

Figure 1-2: Anatomical schematic of magnetoplasma rocket (VASIMR) engine.

1.4 Anatomy of the VASIMR engine:

The word VASIMR is an abbreviation for Variable Specific Impulse Magnetoplasma Rocket, and it mains that VASIMR can vary its specific impulse. The helicon plasma source, the magnetic nozzle, and the ICRH plasma accelerator make up the three main components of the VASIMR engine. The three stages are connected by the external magnetic field, which also passes via the magnet assembly and transmits the ship-propelling exhaust reaction forces.

In the first process, the combined helicon discharge generates the plasma by heating a propellant, usually a gas, with electromagnetic waves (ionization process). After that, the majority of the ionized plasma energy is added via heating ion cyclotron resonances ICRH (energization process). Finally, the adiabatic expansion of the plasma in a magnetic nozzle yields axial momentum, whereas this expansion leads to high thrust (acceleration and detachment process)(figure (1-2)).

The Figure (1-3) shows the different parts of VASIMR engine. The power source antenna receives a propellant that is fed there and ionized. After that, the cold plasma is directed toward the RF (an electromagnetic wave has a low frequency range of around 20 kHz to around 300 GHz.) helicon antenna, where it is heated and activated. After then, it exits through the

magnetic nozzle and accelerates there. To produce thrust further downstream, the ions must separate from the magnetic field.

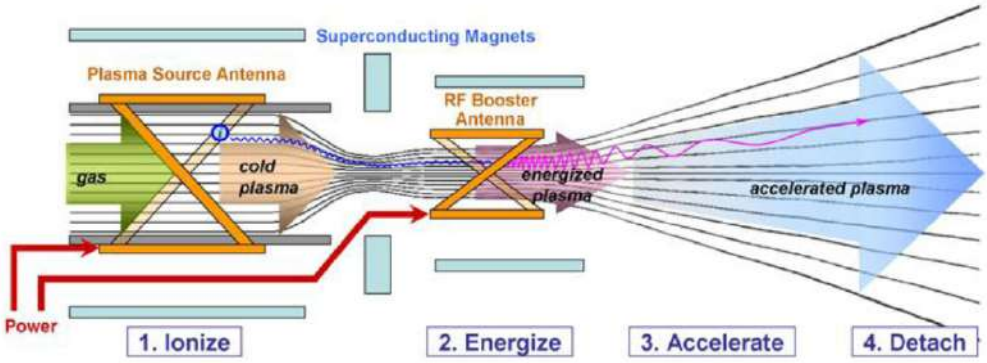

Figure 1-3: Different parts of VASIMR engine.

A VASIMR engine process consists of three main subsystems: the nozzle, the heating stage, and the injection stage.

1.4.1 Injection Stage (Helicon Discharge):

In the plasma generator stage, an excitation of plasma by helicon waves (a low-frequency electromagnetic wave) produced by radio frequency heating is known as a helicon discharge. This magnetic field produces a helicon mode of operation that has a higher electron density and ionization efficiency. Physical electrodes are needed for the majority of plasma rockets, and these soon degrade in the hostile environment. By contrast, radio antennae are used in VASIMR. Similar to how food is heated in a microwave oven, the radio waves heat the plasma. Two-wave mechanisms come into play: First, helicon waves cause the neutral gas in the injector stage to create dense, relatively cold (approximately $60,000$ K) plasma (VASIMR, 2009, 241008) [8, 9]. These oscillations are electromagnetic in their physic nature, occurring between 10 and 50 MHz.

The radio frequency heating is produced by an RF generator that converts the direct current power (DC power) to RF power and performs impedance matching between the RF generator

output and the rocket core (figure (1-4)).

The RF generator of VX200−1 can create [10]:

- RF: 48 ± 1 kW.

- Efficiency: $91 \pm 1\%$.

while the RF generator of VX200−2 can create [10]:

- RF: 172 ± 1 kW.

- Efficiency: $98 \pm 1\%$.

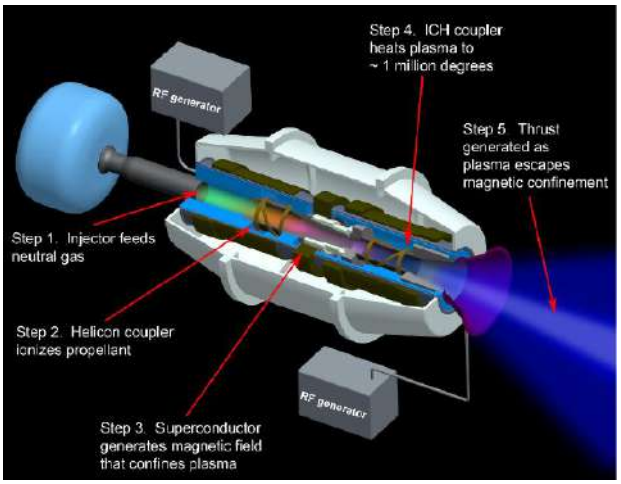

Figure 1-4: Schematic showing the position of the two RF generators in the VASIMR® VX-200.

The first stage contains three main elements: selection of propellant, injector, and helicon.

A- Selection of propellant:

Four distinct propellant gasses are available for usage in the particular mission (table (1.1)). Under certain circumstances, these four gases can be transformed into plasma [13].

.

Gases such as argon, neon, hydrogen, and xenon have potential uses. The table (1.1) shows that the characteristics and properties of each gas are not the same. It appears that any of the mentioned gases can be used after observing and taking into account all of the potential qualities of each gas. The principal Weight and cost are major considerations in these kinds

Table 1.1: Some properties and parameters of the four propellants used in plasma VASIMR engine.

Propellant	Argon(Ar)	Xenon(Xe)	Hydrogen(H)	Neon(Ne)
Properties				
Atomic Weight	39.948	131.3	1.0079	20.179
Atomic Volume(cm3/mol)	22.4	37.3	14.4	16.7
Density @293K(g/cm3)	0.001784	0.00588	0.0000899	0.0009
State	gas	gas	gas	gas
Melting Point (K)	83.85	161.3	14.01	24.53
Boiling Point (K)	87.3	165	20.28	27.1
Specific Heat Capacity(J/gK)	0.52	0.158	14.304	0.904
Heat of vaporozation(kJ/mol)	6.447	12.636	0.904	1.7326
Heat of fusion(kJ/mol)	1.188	2.297	0.117	0.3317
1st Ionization Energy(kJ/mol)	1520.5	1170.4	1312	2080.6
2nd Ionization Energy(kJ/mol)	2665.8	2046.4	-	3952.2
3rd Ionization Energy(kJ/mol)	3930.8	3097.2	-	6121.9
Thermal Conductivity(W/mK)	0.0177	0.00565	0.1805	0.05
Cost in $ (/100g)	0.5	120	12	33
Ionization Energy/Cost (eV)	100	80	200	150

of rocket design projects. Argon is the least expensive gas accessible, as the table illustrates. Xenon costs over 1200 $/ kg, while argon costs about 50 $/ kg. Here, argon is employed in the intended mission.

B-Injector:

One of the most crucial components of the engine is the injector, since it is where the engine's operation begins [14]. Here, the flow of gas from the tank is controlled using a Moog-style flow controller (figure (1-5)). It serves as an injector with a 150 mg/ s propellant flow rate capability. The injector is capable of the following specialized performances:

- Flow rate: from 5 to 100 l/ min.

- Maximum flow: about 180 l/ min where (47 g/ min = 783 mg/ s).

It is important to mention here that the output flow of the moog-type flow controller is within a radius of approximately one to four cm.

Figure 1-5: Moog type flow controller.

c-Helicon Stage:

The engine's real propulsion phase begins at the helicon stage. It raises the temperature of the gas that is moving across the vacuum area between the two ends of coils. The helicon is a 16 cm long helical antenna that has an 11 cm breadth distributed along its length [8, 9].

A very high-quality glass tube is made of 4 cm in diameter, and inserted in the helicon antenna, which can bear the high temperatures (figure(1-6)). Figure (1-7) below shows the actual helicon antenna when mounted and used in the VASIMR engine test. It shows the helicon antenna mounted in the open space between the magnetic mirrors.

The power used to run the helicon stage is 30 kW. This step involves heating the argon gas to the point where plasma is produced.The engine's ICRH is reached by the cold plasma as it passes through the engine.

1.4.2 The Heating Stage (ICRH-Ion Cyclotron Resonance Heating):

In the ICRH step, the energy is transmitted to the plasma in the form of a circularly polarized RF signal that is characterized by the ion cyclotron frequency (figure (1-8)). The reason ICRH heating is used is that it directly provides energy to the plasma ions, which increases engine efficiency. The movement of ions in a magnetic field is connected to a phenomenon called ion

Figure 1-6: Steady-state of the actual discharge source of the helicon.

Figure 1-7: Actual source of Helicon antenna.

cyclotron resonance [18]. The frequency of a charged particle moving perpendicularly to the direction of a uniform magnetic field $\overrightarrow{B} = cte$ (magnetic field has a constant amplitude and direction) is known as the cyclotron frequency. In this case, the acceleration of ion cyclotron resonance increases the temperature of flowed plasma. This latter gets the maximum thermal energy at this stage. Thus, the plasma particles will be exhausted out through the magnetic nozzle to get the thrust.

The energy cost absorbed in this step is 160 to 170 kW of electric power. Similarly to the injection stage, an antenna is designed with different structures and dimensions to heat the plasma and achieve good efficiency:

- width: 11 cm
- length 20 cm.

Figure 1-8: Actual image of the ICRH antenna in VASIMR.

Depending on the modification of both the angle of twist and the number of straps, some previous work has been done on the ICRH antenna to achieve the most efficiency (figure (1-9) and table (1.2)).

.

The most efficient ICRF antenna can give 66% of efficiency with 0 degree twist in the antenna structure [20].

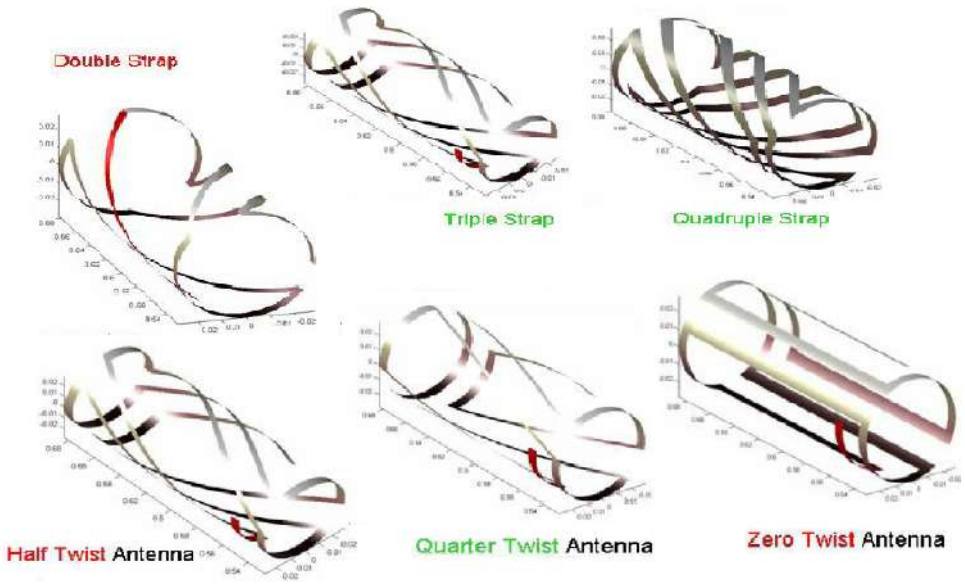

Figure 1-9: Some previous improvement for ICRH antenna.

Table 1.2: Comparisons between some experimental results of antenna geometry.

Antenna Geometry	Ion Loading	Electron Loading	Efficiency (%)
Double Strap, half twist	70	50	39
Triple Strap, half twist	138	96	54
Quadruple Strap, half twist	149	197	63
Half twist	138	96	54
Quarter twist	152	168	62
Zero twist	134	262	66

Magnetic Mirror:

The magnetic mirror is a dispositive permit to confine a plasma or ionized gas, so it known as a pyrotron or magnetic traps. Two ring electromagnets with the same direction of current flow create the simplest magnetic mirror. In the vicinity of the rings, the magnetic field is confined, but it expands between them. The mirror performed when the charged particles spiraling into a converging the line of magnetic field. Along field lines, charged particles move in a helix, rotating around them at the so-called cyclotron frequency and the Larmor radius [21].

A particle's perpendicular velocity increases as it gets closer to a tighter, stronger field, while its parallel velocity decreases proportionately to maintain a constant total energy. The direction of the force the field applies to the particle explains why. The direction of the field and the particle's velocity are always perpendicular to the force. The force is radial and has no effect on the parallel velocity near the mirror's center, where the field lines are parallel [22]. However, when the particle approaches the constriction, the force tilts away from it, creating an imbalance that causes the particle to slow down and recoil. The opposite of the field's influence occurs when the particle is leaving the constriction, causing it to accelerate. Rotational motion is sacrificed in order to achieve acceleration since no additional energy is used. The particle is not affected by the magnetic field; rather, it is merely a means of allowing this energy transfer [23].

In order to protect the engine material from damage due to the high temperature of the hot plasma, we must provide strong confining magnetic fields. For this purpose, two kinds of magnets are available for use in the VASIMR engine. The first is BSCCO (Bismuth Strontium Calcium Copper Oxide). It has suitable properties:

- high power superconducting compound.
- withstand high temperature operating environment.
- able to induce a magnetic field reaching 3 T.

and it is made of:

- 8 superconducting pancake set, assembled under an axial compression load.
- about 500 turns.
- current passing through 110 amps.

1.4.3 Magnetic Nozzle:

After adding energy to the plasma by Ion Cyclotron Resonance heating, the plasma will be immediately ejected and then expanded, in the last part of VASIMR, by a magnetic nozzle that directs the plasma particle path into the axial thurst instead of the radial one [24, 25, 26]. At this current stage, the magnetic field lines are diverging, which makes the field able to transist the thermal energy into kinetic energy as well as protect the thurster surface [27, 28, 29]. This is the stage where the plasma partucles are detached from the magnetic field, thus creating thurst [30, 31, 32].

Currently, the numerous plasma propulsion systems have been devoloped and tested in the relatively small vacuum chamber on Earth [33] compared to the actual area in which the detachment step can act. When the engine is tested in space, we can determine if the plasma will detach from the magnetic field or not.

1.5 Performance of VASIMR:

Ionization cost E_i, which is expressed as energy per ion in terms of electron volts, is the word that is most frequently used to describe the efficiency of plasma formation. The propellant is fed into the upstream end of the VASIMR helicon section and flows to the ICH section. Every ion loses one electron due to the RF power $P_{1,RF}$. The ionization cost is given by,

$$E_i = \frac{P_{1,RF}}{\frac{\dot{m}}{m_p}} - E_1 \tag{1.1}$$

where E_1 is the kinetic energy carried by ions, m_p is the propellant mass, and $\dot{m}$ is the propellant flow rate.

The whole RF power linked to plasma is divided by the thruster jet power to find the

$VX-200$ thruster efficiency. The definition of jet power is

$$P_{jet} = \frac{F^2}{2\dot{m}} \tag{1.2}$$

where $\dot{m}$ is the total mass flow rate of propellant and F is the overall force generated by the rocket. Using a force impact target that assessed the local force density within the exhaust plume as a function of radial position, the force from $VX-200$ was ascertained.

The jet power is divided by the coupled total RF power to determine the thruster efficiency.

$$\eta_T = \frac{P_{jet}}{P_{1,RF} + P_{2,RF}} \tag{1.3}$$

where the RF power connected to the first and second stage plasmas is denoted by $P_{1,RF}$ and $P_{2,RF}$, respectively.

Using the total force measurement and the propellant mass flow rate measurement, the specific impulse was computed as follows:

$$I_{sp} = \frac{F}{\dot{m}g} \tag{1.4}$$

where

$$P_{jet} = \frac{\dot{m}g^2}{2} I_{sp}^2 \tag{1.5}$$

1.6 Conclusion:

The VASIMR engine in a plasma rocket has 10 times the performance of a chemical engine. This result is due to the absence of an electrode touching the hot plasma, which leads to neglecting erosion (issues that other varieties of electromagnetic rockets encounter) and contributes to increasing the lifetime of the engine. Another aspect that can increase the lifetime and power

density is that the magnetic field protects the surface of the rocket from the hot plasma. Because VASIMR requires a vacuum to function and has a low thrust to weight ratio, it is not appropriate for launching payloads from Earth's surface. Rather, it would serve as a cargo upper stage, which would lower the amount of fuel needed for in-orbit travel.

Chapter 2

Generality on plasmas

2.1 Introduction:

When exposed to a heat source, plasma, also known as the fourth state of matter, first liquefies, then transitions to the gas state, and finally forms a plasma [35]. American scientist I. Langmuir coined the term "plasma" in 1928 and used it for the first time in physics [36].

The plasma contains free-moving electrons and ions in all directions in space. The nature of the interaction between charged particles in a plasma sets it apart from a typical gas that contains only electrically neutral particles [37].

2.2 Degree of ionization:

The degree of ionization of plasma is defined as the ratio (from 10^{-10} to 1) [38]

$$\alpha = \frac{N_i}{N_i + N_0} \tag{2.1}$$

where

N_i is the density of electrons (or positive ions).

N_0 is the density of the neutrals.

2.3 Plasma Parameters:

In order to provide a more precise description of the physical phenomenon, we mention the most significant parameters.

2.3.1 Plasma Frequency:

Because electron displacement can disturb an initially neutral plasma, it can be said that electron movement joins oscillations around the equilibrium position. As a result of this excess movement, an electron appears from a small distance (compared to the length of Debye λ_D). The plasma frequency ω_{pe}, which characterizes the time scale, can be found using the following formula [38]:

$$\omega_{pe} = \left(\frac{N_e q_e^2}{m_e \varepsilon_0}\right)^{1/2} \tag{2.2}$$

With N_e the electron density of uninterrupted plasma (initial), q_e the charge of an electron, m_e the mass of an electron, and ε_0 the dielectric constant.

The numerical form of ω_{pe} in Hz is:

$$\omega_{pe} = 5.64 \times 10^4 {N_e}^{1/2} (\text{CGS}) \tag{2.3}$$

N_e : the electron density of plasma, expressed $\left(\text{en cm}^{-3}\right)$.

From ω_{pe} we can indicate, the characteristic time of the plasma T_{pe}:

$$T_{pe} = 2\pi/\omega_{pe} \tag{2.4}$$

The response time of an excitated plasma is a time in the order of ω_{pe}^{-1}[38].

2.3.2 Debye Length:

The average distance after which the disturbance caused by the ion's existence is screened by the electrons is known as the Debye length, or λ_D [37]

$$\lambda_D = \sqrt{\frac{\varepsilon_0 k_B T}{q_e^2 N_e}} \tag{2.5}$$

Given the expressions for the plasma temperature T in K and N_e in cm^{-3}, the following formula yields λ_D

$$\lambda_D \approx 6.9(T_e / N_e)^{1/2}(\mathrm{CGS}) \tag{2.6}$$

2.3.3 Landau length: (Critical length of binary interaction):

Analysis of collision events and position correlations in a plasma both use Landau's length.

$$k_B T = \frac{e^2}{4\pi\varepsilon_0 r_0} \tag{2.7}$$

Hence:

$$r_0 = \frac{q_1 q_2}{4\pi\varepsilon_0 k_B T} \tag{2.8}$$

with k_B is the Boltzmann constant and T is the medium temperature.

We can observe that r_0 is the distance that two electrons must travel to get close enough to one another for their potential energy of binary interaction to equal their kinetic energy of thermal agitation.

2.3.4 Ratius of the ionic sphere:

R_s is the radius of the central sphere in the plasma that is occupied by a moving ion. The radius is provided by [39]

$$R_s = \left(\frac{3}{4\pi N_i}\right)^{1/3} (\mathrm{CGS}) \tag{2.9}$$

with N_i is plasma ion density $\left(\text{in } \mathrm{cm}^{-3}\right)$.

2.3.5 Electronic sphere radius:

The unique average dimension of two electrons is the radius of the electron sphere. The relationship that follows defines it [40].

$$R_s = (\frac{3}{4\pi N_e})^{1/2} \tag{2.10}$$

with N_e the electron density of the plasma $\left(\text{in } \text{cm}^{-3}\right)$.

2.3.6 De Broglie Thermal Wave Length:

It is defined as follows and provides an approximation of the quantum nature of plasma particles:

$$\lambda_t = \left(\frac{2\pi\hbar^2}{mk_BT}\right)^{1/2} (\text{CGS}) \tag{2.11}$$

where m is the mass of the particle.

2.4 Plasma in a constant uniform magnetic field:

The movement of a free charged particle in a magnetic field constant (i.e. not varying over time) is determined by the Lorentz force which is perpendicular to both the speed $\mathbf{v}$ of the particle and the magnetic field B. If we assume the movement is not relativistic, the equation of motion is:

$$m\frac{d\mathbf{v}}{dt} = q(\mathbf{v} \times \mathbf{B}) \tag{2.12}$$

where q its charge and B is the magnetic field vector. By multiplying scalarly both sides of this equation by $\mathbf{v}$ we obtain:

$$\frac{d}{d\mathbf{t}}(\frac{mv^2}{2}) = 0 \tag{2.13}$$

That is to say:

$$\frac{mv^2}{2} = \varepsilon = cte \tag{2.14}$$

Thus, kinetic energy ε of a charged particle deploying into a static magnetic field is constant and this irrespective of the spatial dependency $\mathbf{B}(\mathbf{r})$ of that field.

Suppose now that the magnetic field is not static settlement but also uniform (independant de r). The equation (2.12) can then also be written:

$$\frac{d\mathbf{v}}{dt} = \mathbf{\Omega} \times \mathbf{v} \tag{2.15}$$

or we introduced the constant vector, called cyclotron frequency:

$$\mathbf{\Omega} = -\frac{q}{m}\mathbf{B} \tag{2.16}$$

The equation (2.15) is a classical equation of a vector $\mathbf{v}$ anime of a rotation around an axis. To be able to write equations valid for both electrons and ions, we also introduce the algebraic value of the cyclotron frequency

$$\overline{\Omega} = -\frac{q}{m}B \tag{2.17}$$

or $\mathbf{B}$ is assumed positive.We can now show that the most general trajectoryof a particle is a helix obtained by superposition of the rotation around and a translation $\mathbf{\Omega}$ has the speed $v_{\|}$ in the direction of $\mathbf{\Omega}$. For this, take the Oz axis as an axis parallel to $\mathbf{B}$ and oriented in the same sense. The movement in the z direction is therefore:

$$v_z = v_{\|} = cte \tag{2.18}$$

$$z = z_0 + v_{\|}t \tag{2.19}$$

In x and y directions, equations can be combined in writing. So we have:

$$v_x = v_{\perp}\cos(\overline{\Omega}t + \varphi) \tag{2.20}$$

$$v_y = v_{\perp}\sin(\overline{\Omega}t + \varphi) \tag{2.21}$$

$$v_x^2 + v_y^2 = v_{\perp}^2 = cte \tag{2.22}$$

so that perpendicular energy remains constant as requires equation (2.14). The position of

the particle is obtained by integration

$$x = X_0 - \overline{\rho}\cos\alpha(\overline{\Omega}t + \alpha) \tag{2.23}$$

$$y = Y_0 + \overline{\rho}\sin\alpha(\overline{\Omega}t + \alpha) \tag{2.24}$$

$$x = x_0 - \overline{\rho}\cos\alpha \tag{2.25}$$

$$y = y_0 + \overline{\rho}\sin\alpha \tag{2.26}$$

$$\overline{\rho} = \frac{v_\perp}{\Omega} \tag{2.27}$$

In general, the particle has a non-zero initial speed parallel to **B** and the trajectory in space is a helix, like the one represented on Figure (2-1).

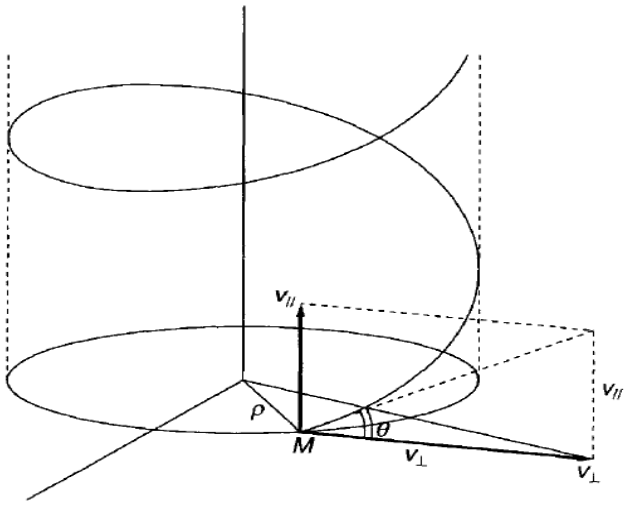

Figure 2-1: Helicoidal trajectory for ρ Larrnor radius, and θ angle of inclination.

2.5 Conclusion:

Plasma can be considered a strong source of renewable energy; it derives its energy from fast particles. To benefit from the high energy of ionized gas, we must be aware of all the properties of plasma. In the next chapter, we will explain one of the modern uses of plasma energy for space purposes.

Chapter 3

Results and discussions

3.1 Introduction:

This chapter contains two purposes that underlie our investigation and can lead us to competence improvement. Firstly, we have treated numerically the evolution of efficiency in the magnetic nozzle stage of VASIMR (VF-24). According to the wide range of VISMIR parameters (electron temperatures, densities, spectroscopic charge numbers, and exhaust size), we have determined the perfect parameter ranges for the maximal values of efficiency. Then, we have tried to apply our derived formulas that they have never calculated before to a recent research and estimate our correction in this case.

3.2 The VASIMR thruster (VF-24):

The efficiency of VASIMR has usually been calculated by:

$$\eta_T = \frac{P_{jet}}{P_{1,RF} + P_{2,RF}} \tag{3.1}$$

where the RF power connected to the first and second stage plasmas is denoted by $P_{1,RF}$ and $P_{2,RF}$, respectively.

At the magnetic nozzle stage on the VASIMR competence, a new criterion can be introduced in our estimation and denoted as $L(\%)$

Table 3.1: Interesting typical values of operating parameters for 24 kW VASIMR thruster.

	Operating parameter	**Definition**	**Typical value**
1	Input power	$P = P_{1,RF} + P_{2,RF}$	$24,000(\,\mathrm{W})$
2	Power efficiency	η_T	40%
3	ion temperature	T_i	$10 - 100(\,\mathrm{eV})$ or $1.160\,4 \times 10^5 - 1.160\,4 \times 10^6\,(\,\mathrm{tmpK})$
4	Electron temperature	T_e	$1 - 10(\,\mathrm{eV})$ or $11604. - 1.160\,4 \times 10^5\,(\,\mathrm{tmpK})$
5	Average ion density at the exhaust	n_a	$0 - 2 \times 10^{18}(\,\mathrm{m}^{-3})$
6	Radius of plasma at the end-exhaust.	$r_{\max}$	$1(\,\mathrm{m})$

We take into consideration for both electrons and ions at the nozzle $L_i(\%)$, $L_e(\%)$

where

$$P_{Bi} = \frac{dw_i}{dt} \tag{3.2}$$

$$P_{Be} = \frac{dw_e}{dt} \tag{3.3}$$

Using 24 kW of direct current electric power, the VASIMR system is currently being developed for the first space flight experiment. The 24 kW VASIMR thruster (VF-24) have the operational parameters shown in Table (3.1)[24].

Firstly, we should deduce the jet power of the third stage in VASIMR

$$P_{jet} = (P_{1,RF} + P_{2,RF})\,\eta_T = 9600(\,\mathrm{W}) \tag{3.4}$$

We have drawn the percentage $L(\%)$ for the 24 kW VASIMR thruster (VF-24) according to the conditions and concentrations in Table (3.1), and we have assumed a probability that $0.001 < x < 0.02$.

3.2.1 The influence of the volume dimensions:

The figures (3-1) and (3-2) show the variations of percentages $L_e(\%)$ and $L_i(\%)$ as a function of volume parameters $r_{\min}$ and x. We notice that both the electronic and ionic corrections are growing with increasing length x and decreasing with increasing minimal radius $r_{\min}$.

3.2.2 The influence of both density and temperature:

In the situation where $r_{\min} = 0.6\,\mathrm{m}$, $x = 0.02$ m, the percentage fluctuations of $L_e(\%)$ and $L_i(\%)$ as a function of electronic temperature T_e and density n_a are depicted in the figures (3-3) and (3-4). We observe that when the electronic temperature and density increase, so do the ionic and electronic corrections.

Table 3.2: Interesting typical values of operating parameters for 24 kW VASIMR thruster.

	Operating parameter	**Definition/Typical value**
1	Input power	$P = P_{1,RF} + P_{2,RF} = 24,000(\,\mathrm{W})$
2	Power efficiency	$\eta_T = 0.4$
3	spectroscopic charge number	$Z = 2$ (Propellant is Deuterium)
4	ion energy	$W_i = 100(\,\mathrm{eV})$
5	Electron temperature	$T_e = 5(\,\mathrm{eV}) = 58022\,(\,\mathrm{tmpK})$
6	Average ion density at the exhaust	$n_a = 10^{18}(\,\mathrm{m}^{-3})$
7	Radius of plasma at the end-exhaust.	$r_{\max} = 1(\,\mathrm{m})$

3.2.3 The influence of the atomic number:

The percentage fluctuations of $L_e(\%)$ and $L_i(\%)$ as a function of atomic number Z is shown in figures (3-5) and (3-6). We note that the ionic and electronic corrections grow with the atomic number.

3.3 Power in work of A.V. Ilin and al:

We have calculated the percentage $L(\%)$ for the previous published study of the A.V. Ilin [24]. We have explored the conditions and concentrations of this publication and exploited them to calculate the percentage of the thruster efficiency. We also take into consideration both electrons and ions at the nozzle.

Using the kinetic energy of the ion, we can deduce its temperature.

$$T_i = \frac{2}{K_B} W_i = 2.320\,9 \times 10^6\,\mathrm{K} \tag{3.5}$$

Now we apply all the above values to our expression of the radiation loss.

$$L_e(\%) = 6.344\,0 \times 10^{-5} \tag{3.6}$$

$$L_i(\%) = 6.419\,8 \times 10^{-3} \tag{3.7}$$

$$P_{Be}\,\max = 6.090\,2 \times 10^{-3}\,\mathrm{W} \tag{3.8}$$

$$P_{Bi}\,\max = 0.616\,3\,\mathrm{W} \tag{3.9}$$

3.4 Conclusion:

In this chapter, we have used a good argument to find perfect ranges of concentrations within which the efficiency will be strong. The improvement in the efficiency of VASIMR rocket depends on the specific range of conditions. In the case of 24 kW VASIMR, we suggest a high temperature and density for plasma with low atomic number.

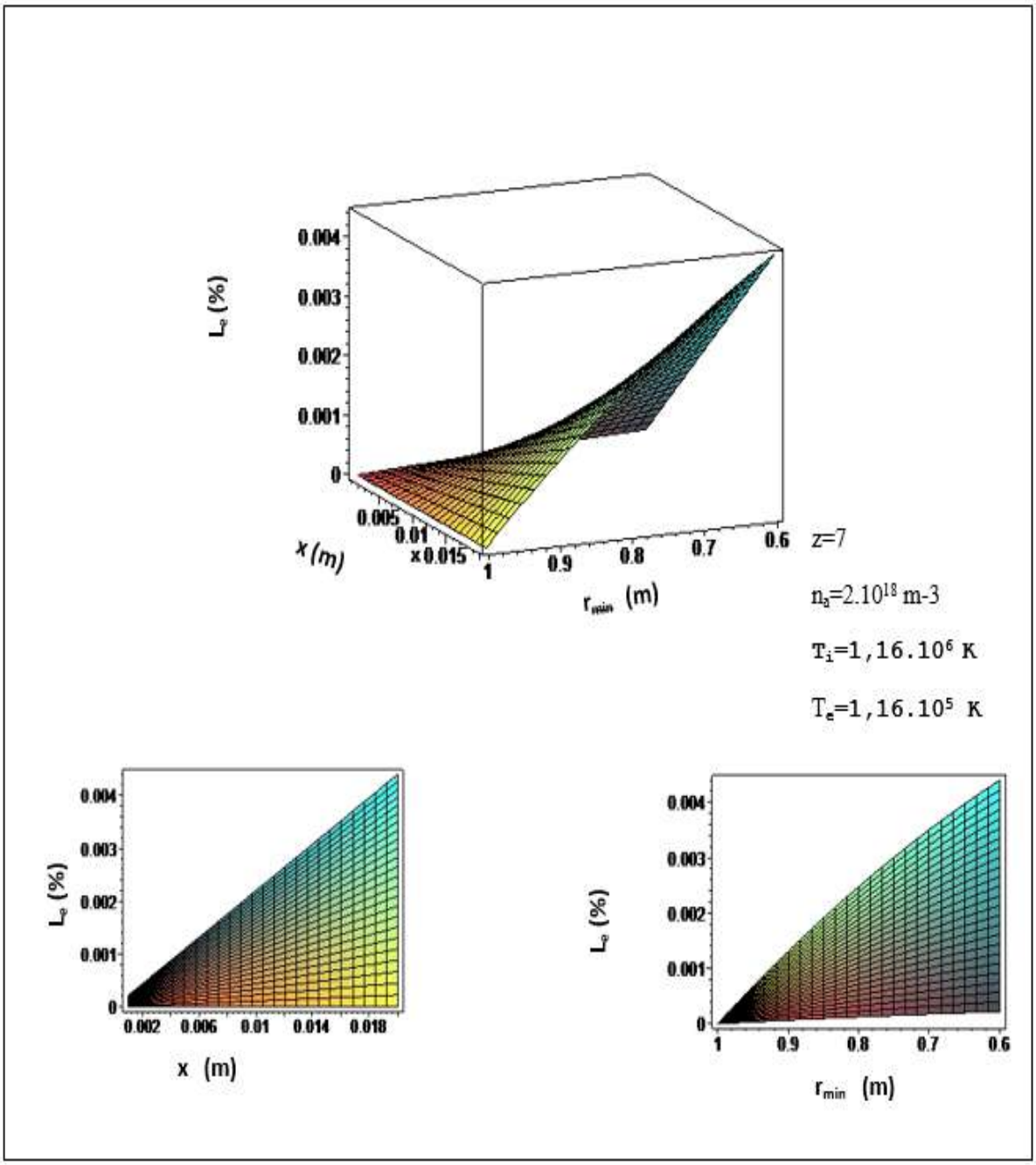

Figure 3-1: Evolution of percentage $L_e(\%)$ as a function of volume parameters $r_{\min}$ and x in the case where $n_a = 2.10^{18}\,\mathrm{m}^{-3}$, $T_e = 1.16 \times 10^5$ K, and $z = 7$.

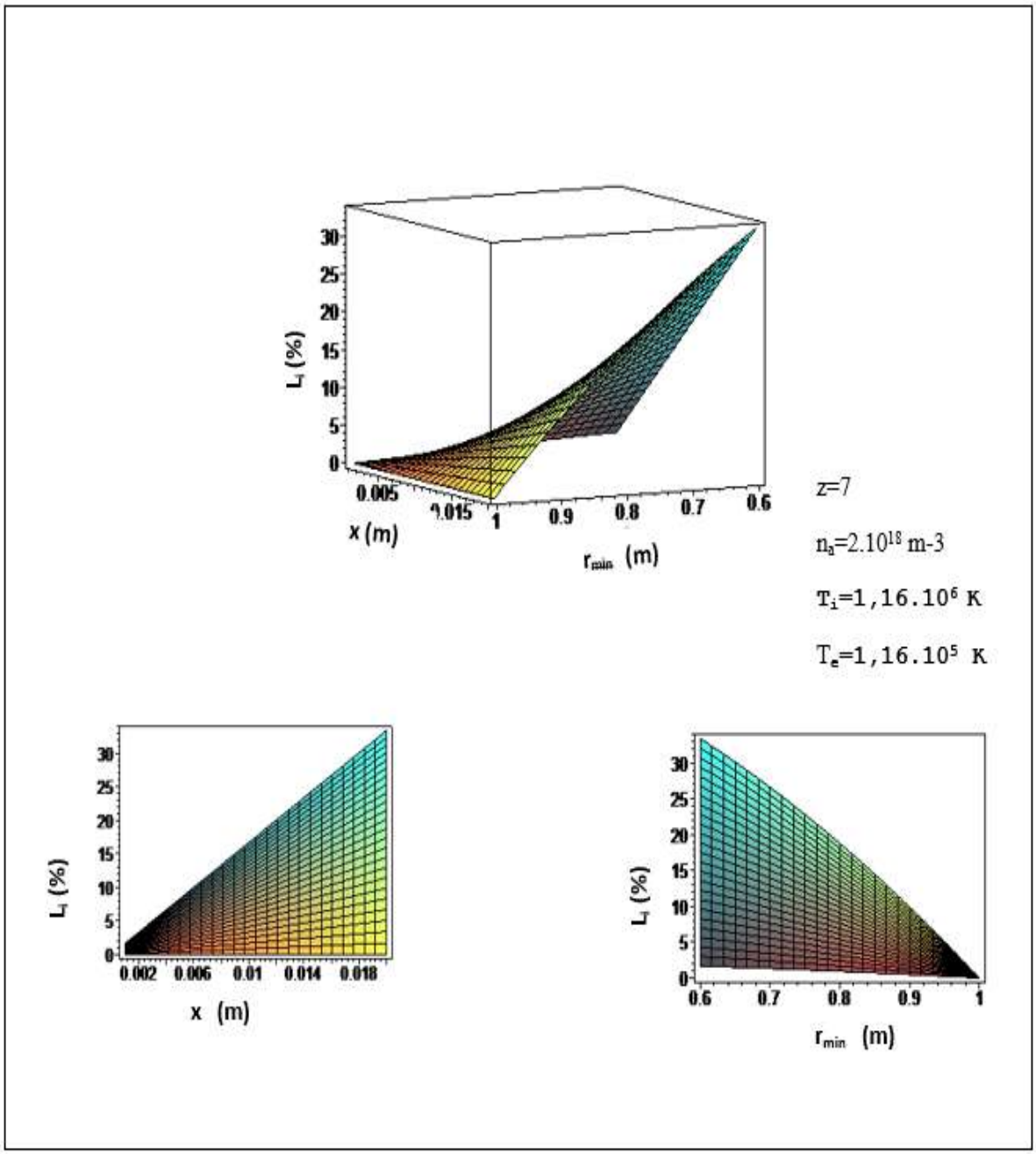

Figure 3-2: Evolution of percentage $L_i(\%)$ as a function of volume parameters $r_{\min}$ and x in the case where $n_a = 2.10^{18}\,\mathrm{m}^{-3}$, $T_i = 1.16 \times 10^6\,\mathrm{K}$, and $z = 7$.

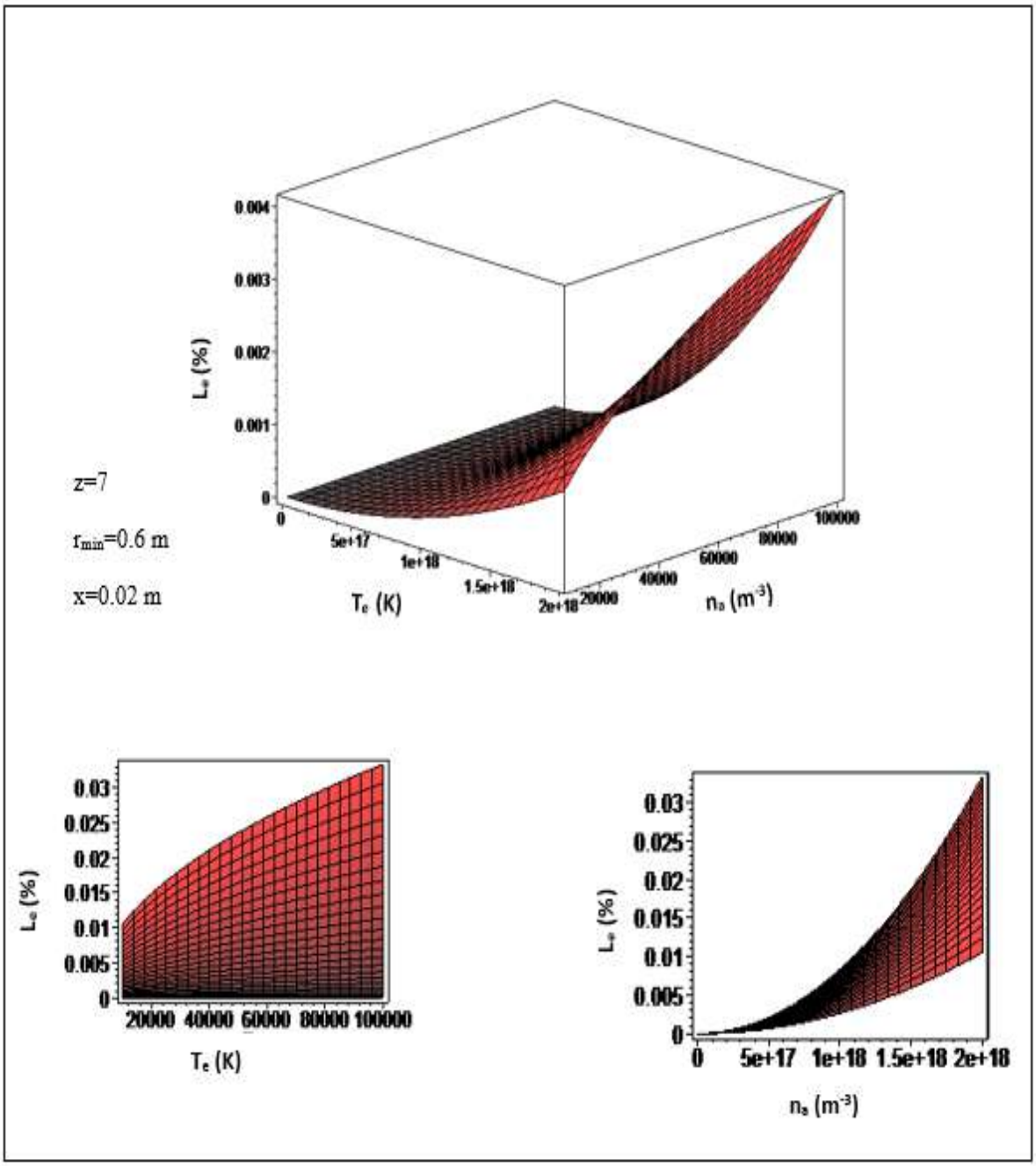

Figure 3-3: Variation of percentage $L_e(\%)$ as a function of electronic temperature T_e and density n_a in the case where $r_{\min} = 0.6\,\mathrm{m}$, $x = 0.02$ m, and $z = 7$.

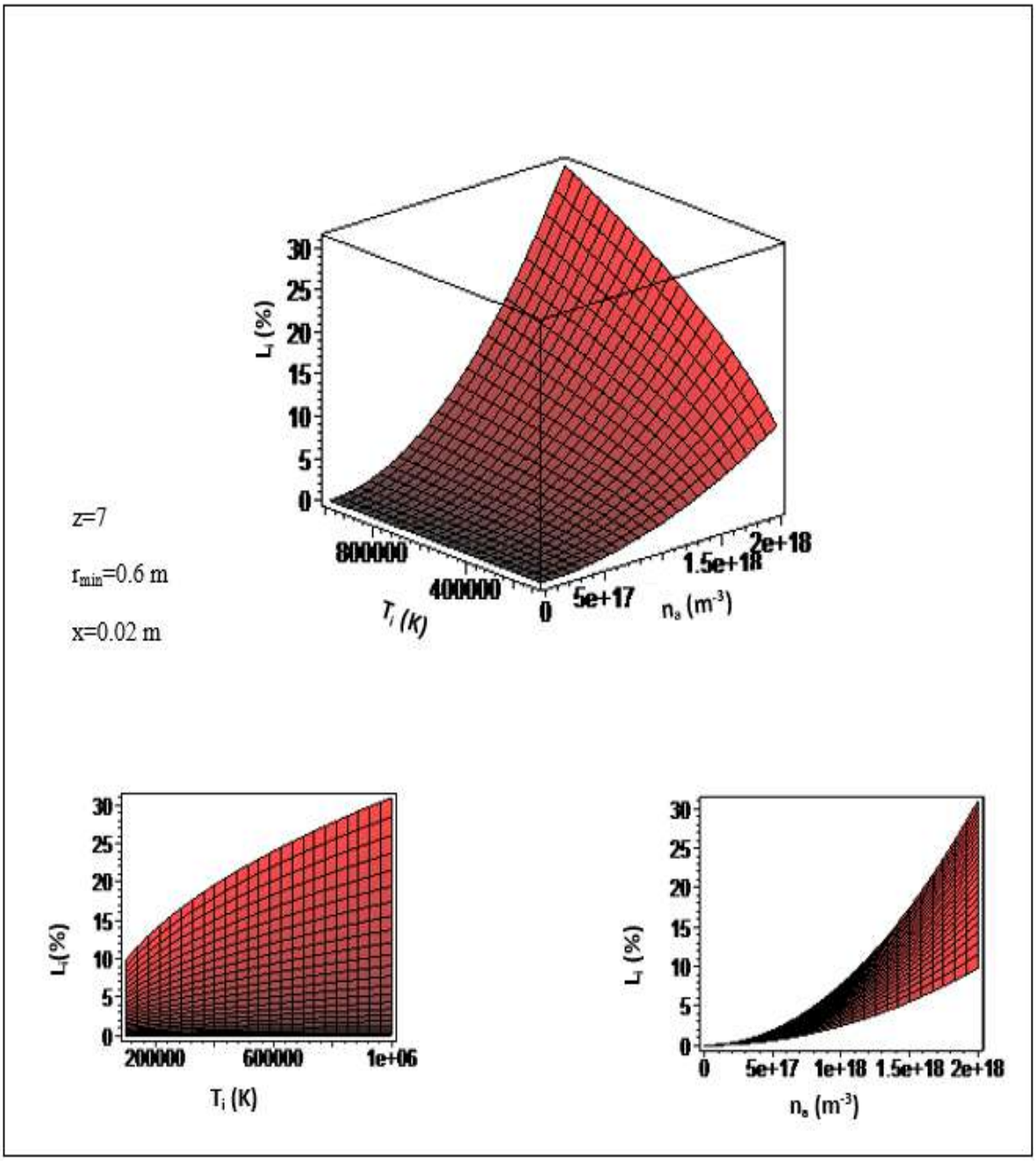

Figure 3-4: Variation of percentage $L_i(\%)$ as a function of ionic temperature T_i and density n_a in the case where $r_{\min} = 0.6\,\mathrm{m}$, $x = 0.02$ m, and $z = 7$.

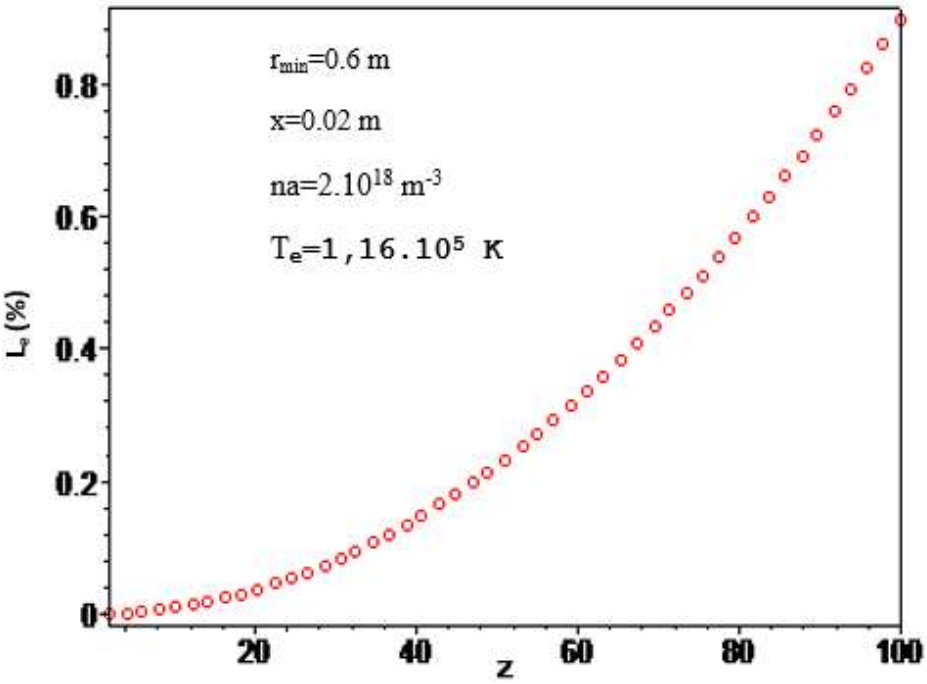

Figure 3-5: Evolution of percentage $L_e(\%)$ as a function of atomic number Z in the case where $n_a = 2.10^{18}\,\mathrm{m}^{-3}$, $T_e = 1.16 \times 10^5$ K, $r_{\min} = 0.6\,\mathrm{m}$, $x = 0.02$ m.

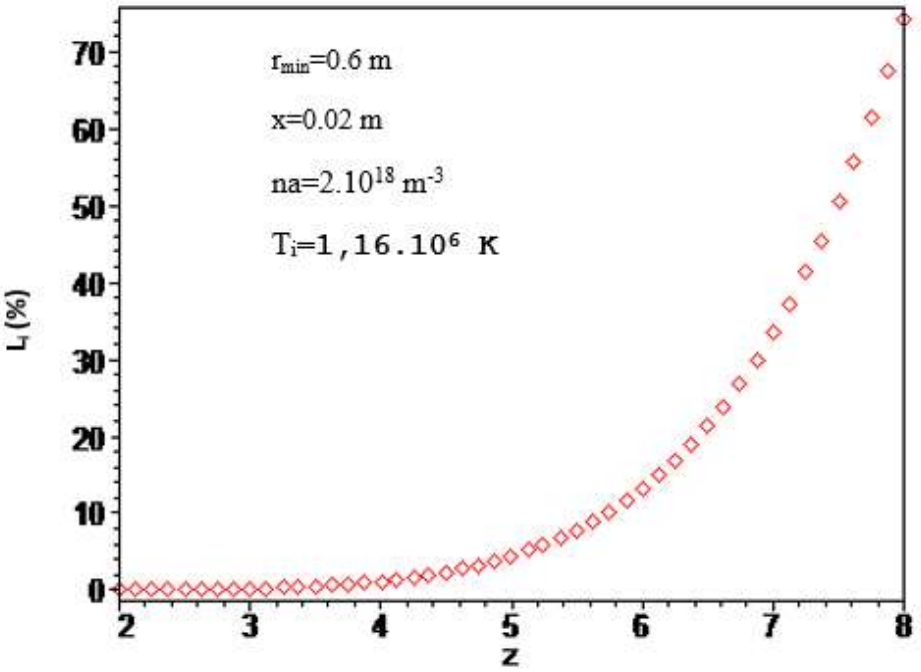

Figure 3-6: Evolution of percentage $L_i(\%)$ as a function of atomic number Z in the case where $n_a = 2.10^{18}\,\mathrm{m}^{-3}$, $T_i = 1.16 \times 10^5$ K, $r_{\min} = 0.6\,\mathrm{m}$, and $x = 0.02$ m.

General conclusion:

Astronaut Franklin Chang Díaz and his scientific team have been working on creating a quicker propulsion technology for space flight since the 1970s, first at MIT and later at NASA.

The VASMIR engine includes the following main steps: processes ionize, energize, accelerate, and detach. In the ionization phase, cold gas enters the process, whereas after detachment, accelerated plasma comes out of the nozzle, which leads to high thrust. Thus, the rocket engine design comes under propulsion.

The power ratio, or the output power (the magnetic nozzle power) divided by the input power (the RF power of the helicon and ICRH systems), should be estimated in order to control the efficiency in the VASIMR. The total input power is determined after accounting for power loss.

Our goal in designing the VASIMR is to control its efficiency by increasing its speed. In the current work, we establish optimal concentration ranges in order to develop a new efficiency improvemnt for the VASIMR engine. The broad range of VISMIR parameters (electron temperatures, densities, spectroscopic charge numbers, exhaust size) has allowed us to identify the ideal parameter ranges for either the optimum efficiency.

We have found ideal concentration levels by using a strong argument. Reducing loss to the lowest feasible level is necessary for the VASIMR rocket to operate more efficiently. We propose a high temperature and density for the light elements (low atomic number plasma) to achieve good efficiency in the 24 kW VASIMR.

Bibliography

[1] Retrieved March 18, 2010, from the NASA/JPL;Website: http://mars.jpl.nasa.gov/odyssey/mission/science/.

[2] Ad Astra Rocket Company. 2012. VF-200. Available: http://www.adastrarocket.com/aarc/VF200 [May 2012].

[3] Andrew V. Ilin*, Franklin R. Chang Díaz†, Jared P. Squire, Plasma Heating Simulation in the TX 77059. Plasma rocket. (2010).

[4] ADAstra rocket company (2010) Retrieved on: August 31,2010 from: www.adastrarocket.com/aarc/Technology.

[5] F. R. Chang-Diaz, J.P. Squire, T. Glover, and A.J. Petro. The VASIMR engine: Project status and recent accomplishments. In 42nd Aerospace Sciences Meeting and Exhibit, 2004.

[6] Ad Astra Rocket Company. 2012 Technology. Available: http://www.adastrarocket.com/aarc/Technology [May 2012]

[7] W. Benjamin. Longmier, P. Jared. Squire, D. Mark. Carter, D. Leonard. Cassady,W. Tim. Glover, J. William. Chancery, S. Chris. Olsen, V. Andrew. Ilin, E. Greg. McCaskill, R.Franklin. Chang Díaz and A. Edgar. Bering, III, Ambipolar Ion Acceleration in the Expanding Magnetic Nozzle of the VASIMR® VX-200i, AIAA. 45 (2009) 5359.

[8] F. F. Chen, "Plasma ionization by helicon waves." Plasma Physics and Controlled Fusion, 33(4), 339-364 (1991).

[9] R. W. Boswell and C. Charles, "The helicon double layer thruster." Presented at the 28th International Electric Propulsion Conference, IEPC 2003, Toulouse, France, 2003.

[10] W. Benjamin. Longmier, P. Jared. Squire, S. Chris. Olsen, D. Leonard. Cassady, G. Maxwell. Ballenger, D. Mark. Carter, V. Andrew. Ilin, W. Tim. Glover, E. Greg. McCaskill, R. Franklin. Chang Díaz and A. Edgar. Bering, III, VASIMR® VX-200 Improved Throttling Range, AIAA. (2012) 3930.

[11] A. Edgar. Bering, III, Matthew Giambusso, Houston and Mark Carter, Andrew Ilin, S. Chris. Olsen, P. Jared. Squire, R. Franklin. Chang Díaz, W. Benjamin. Longmier and W. Benjamin. Longmier, Using VASIMR® for the Proposed Europa Mission, AIAA SPACE 2014 Conference and Exposition. (2014)4344.

[12] S. Christopher. Olsen, G. Maxwell. Ballenger, D. Mark. Carter, R. Franklin. Chang Díaz, Matthew Giambusso, W.Timothy. Glover, V. Andrew. Ilin, P. Jared. Squire and W. Benjamin. Longmier and A. Edgar. Bering, III and A. Paul. Cloutier, An Experimental Study of Plasma Detachment from a Magnetic Nozzle in the Plume of the VASIMR® Engine, IEPC (2013) 123.

[13] A. Edgar. Bering, III and Michael Brukardt, P. Jared. Squire, W. Timothy. Glover, Verlin Jacobson, and Greg McCaskill, Recent Improvements In Ionization Costs And Ion Cyclotron Heating Efficiency In The VASIMR Engine, AIAA Aerospace Sciences Meeting and Exhibit. 44 (2006) 766.

[14] T. Logan. Williams; Ion Acceleration Mechanisms of Helicon Thrusters, University of Michigan, 2013.

[15] http://www.moog.com/images/Products/.

[16] A. Edgar. Bering, III and R. Franklin. Chang Díaz,P. Jared. Squire, W. Timothy. Glover, D. Roger. Bengtson, Michael Brukardt, VELOCITY PHASE SPACE STUDIES OF ION DYNAMICS IN THE VASIMR ENGINE, AIAA. 42 (2004) 150.

[17] Blackwell, D., Chen, F., (1997). 2D imaging of a helicon discharge. Electrical Engineering department, University of California, Los Angeles, California 90095-1594.

[18] A. V. Ilin, F. R. Chang Díaz, J. P. Squire, B. N. Breizman, M. D. Carter, PARTICLE SIMULATIONS OF PLASMA HEATING IN VASIMR, AIAA. 36 (2000) 3753.

[19] V. Andrew. Ilin, R. Franklin. Chang Diad, P. Jared. Squire, D. Mark. Carter, Plasma Heating Simulation in the VASIMR System, AlAA Aerospace Sciences Meeting and Exhibit. 43 (2005) 949.

[20] Glover, T., Diaz, F., Squire, J., Jacobson, V., Chavers, D., Carter, M., (2000) Principal VASIMR Results and Present Objectives. NASA ASPL, TX 77059.

[21] J. L. Delcroix et A. Bers; "Physique des Plasmas", inter édition, CNRS éditions, paris, (1994).

[22] A. V. Burdakov, A. A. Ivanov, E. P.Kruglyakov, PROGRESS IN STUDIES OF MAGNETIC MIRRORS AND THEIR PROSPECTS.

[23] Chang, F.(2010). The VASIMR. Scoentific Americal, 283(5), page: 90-97.

[24] A. V. Ilin, F. R. Chang Díaz, J. P. Squire, A. G. Tarditi, B. N. Breizman, M. D. Carter, SIMULATION OF PLASMA DETACHMENT IN VASIMR, AIAA. 44 (2002) 346.

[25] H. Frans. Ebersohn, W. Benjamin. Longmier, J. P. Sheehan, V. John. Shebalin, S. Sharath. Girimaji, Preliminary Magnetohydrodynamic Simulations of Magnetic Nozzles, IEPC. 33 (2013) 334.

[26] R. Kawabuchi,Matsuda, Y. Kajimura , H. akashimaY .P. Zakharov, umerical Simulation of Plasma Detachment from a Magnetic ozzle by using Fully Particle-In-Cell Code,IFSA. (2008) 112.

[27] Tomihiko Kojimaa, Taichi Moritab and Naoji Yamamotob, Analysis of plasma detachment in the magnetic thrust chamber using full particle-in-cell simulation, High Energy Density Physics. 36 (2020).

[28] Eduardo Ahedo and Mario Merino, On plasma detachment in propulsive magnetic nozzles, PHYSICS OF PLASMAS 18 (2011).

[29] Johan Hedin; Ion Cyclotron Resonance Heating in Toroidal Palsmas, Universitetsservice US AB ,2001.

[30] Eduardo Ahedo, Double-layer formation and propulsive assessment for a three-species plasma expanding in a magnetic nozzle, PHYSICS OF PLASMAS. 18 (2011).

[31] E. Ahedo and M. Merino,Preliminary assessment of detachment in a plasma thruster magnetic nozzle, AIAA. 46 (2010).

[32] M. Merino and E. Ahedo, Plasma detachment mechanisms in a magnetic nozzle, AIAA. 47(2011) 5999.

[33] Ad Astra Rocket Company. 2012. VX-200. Available: http://www.adastrarocket.com/aarc/VX200 [May 2012].

[34] Jared P. Squire1and al., Steady-state Testing at 100 kW in the VASIMR® VX-200SSTM Project, AIAA Propulsion and Energy Forum, JW Marriott, Indianapolis, Indiana, (2019).

[35] L. Ben mebrouk; Mémoire de Magister Université de Ouargla, (2003).

[36] J. L. Delcroix et A. Bers; " Physique des Plasma "; inter édition, CNRS éditions, paris, (1994).

[37] Michel Moisan ,et Jacques Pelletier,"physique des plasmas collisionionnels",EDP Sciences,France,(2006).

[38] A.NAAM;"Thèse de doctorat",Université de Ouargla, (2015).

[39] S. Ichimaru ; " Plasma Physics " ; Benjamin.Cummings. Publishing Company, Inc, Menlo Park. California, (1986).

[40] S. Sahal-Bréchot, Astron. Astrophys. **2**, 322, (1969).

[41] H. R. Griem; "Plasma Spectroscopy", McGraw-Hill, New York (1964).

Abstract

An electromagnetic propulsion rocket has been designed for the journal space called VASIMR . What matters to us in developing the VASIMR is to increase its speed and thus control its efficiency. This present work contains a new improvement has never calculated before based on recent research on VASIMR efficiency. We have developed a new formula that discriminates the radiation loss in the nozzle stage of VASIMR (VF -24), and we have treated numerically the evolution of power l oss by braking radiation. According to the wide range of VISMIR parameters (electron temperatures, densities, spectroscopic charge numbers, and exhaust size), we have determined the perfect parameter ranges for the minimal values of power loss from braking radiation (the maximal values of efficiency). We have established that the high temperature and density of plasma with a low atomic number lead to good improvement on the VASIMR Rocket. We should also avoid using heavy elements in plasma production.

Keywords: VASIMR Rocket, efficiency, nozzle stage.

ملخـــص

تم تصميم صاروخ دفع كهرومغناطيسي لمساحة المجلة يسمى VASIMR. ما يهمنا في تطوير جهاز VASIMR هو زيادة سرعته وبالتالي التحكم في كفاءته. يحتوي هذا العمل الحالي على تحسين جديد لم يتم حسابه من قبل بناءً على الأبحاث الحديثة حول كفاءة VASIMR. لقد قمنا بتطوير صيغة جديدة في مرحلة الفوهة لـ VASIMR (VF-24)، وقمنا بمعالجة تطور القوة عدديًا. وفقًا لمجموعة واسعة من معلمات VISMIR (درجات حرارة الإلكترون، والكثافات، والعدد الذري، وحجم العادم)، فقد حددنا نطاقات المعلمات المثالية للقيم القصوى للكفاءة. لقد أثبتنا أن ارتفاع درجة حرارة البلازما وكثافتها ذات العدد الذري المنخفض يؤديان إلى تحسن جيد في صاروخ VASIMR. ويجب علينا أيضًا تجنب استخدام العناصر الثقيلة في إنتاج البلازما.

الكلمات المفتاحية: صاروخVASIMR ، الكفاءة، مرحلة الفوهة.

Résumé

Une fusée à propulsion électromagnétique a été conçue pour l'espace journal appelé VASIMR. Ce qui nous importe dans le développement du VASIMR, c'est d'augmenter sa rapidité et ainsi maîtriser son efficacité. Ce travail actuel contient une n ouvelle amélioration jamais calculée auparavant sur la base de recherches récentes sur l'efficacité du VASIMR. Nous avons développé une nouvelle formule qui discrimine la perte de rayonnement dans l'étage de buse du VASIMR (VF -24), et nous avons traité numériquement l'évolution de la perte de puissance par rayonnement de freinage. En fonction de la large gamme de paramètres VISMIR (températures électroniques, densités, nombres de charges spectroscopiques et taille des gaz d'échappement), nous avons détermin é les plages de paramètres parfaites pour les valeurs minimales de perte de puissance due au rayonnement de freinage (les valeurs maximales d'efficacité). Nous avons établi que la température élevée et la densité du plasma avec un faible numéro atomique co nduisent à une bonne amélioration du VASIMR Rocket. Nous devrions également éviter d'utiliser des éléments lourds dans la production de plasma.

Mots clés :VASIMR Rocket, efficacité, étape de buse.